

a craft is ordinarily degraded if hydrofoils of any area are immersed at a craft speed less than the optimum lift-off speed).

4) After a water-conveyance (hydrofoil) craft has reached the optimum lift-off speed, there is no value to be gained by the use of hydrofoils in combination with a partially elevated craft unless there is a significant variation in $(L/D)_h$ due to hydrofoil loading [in fact, the performance of a craft is ordinarily degraded if any portion of the hull(s) is submerged at a craft speed greater than the optimum lift-off speed].

ROBERT M. L. BAKER, JR.
Computer Sciences Corporation and
University of California, Los Angeles

References and Notes

1. B. Chance, Sr., P. DeSaix, H. Herreshoff, J. H. Milgram, *Science* **156**, 412 (1967).
2. H. M. Barkla, *Trans. Roy. Inst. Naval Architects, London* **93**, 247 (1951); K. S. M. Davidson, *Surveys in Mechanics* (Cambridge Univ. Press, London, 1956), p. 473; B. Smith, *The 40-Knot Sailboat* (Grosset and Dunlap, New York, 1963), pp. 1-134; C. A. Marchaj, *Sailing Theory and Practice* (Dodd, Mead, New York, 1964), pp. 305-310; C. Miller, *Rudder* (July 1965), pp. 20-26.
3. Equation 1 is a modification of equation 53, p. 176, of L. Prandtl, *Essentials of Fluid Dynamics* (Haftner, New York, 1952).
4. A conservative and easily achievable $(L/D)_h$ was chosen from data given in R. Altmann, *High-Speed Towed Hydrofoil Sled, Amer. Inst. Aero. Astronaut. and Soc. Nav. Architects and Mar. Engr., Advanced Marine Vehicles Meeting*, May 1967, p. 3 and Fig. 1.
5. W. S. Bradfield, private communication, 5 May 1968.
6. The algebra that results in Eq. 6 is based upon an addition of Eqs. 2 and 3a [where $M/\rho w$ is replaced here by $[Mg - f_{DF} (L/D)_h]/\rho wg$ and $(L/D)_h$ is assumed to include A_p and be a function of craft speed and hydrofoil loading] and a division of this sum by Eq. 2 plus $(1/2) \rho w A_p C_D V^2$. For certain hull forms, k and C_D vary with Δ , and this effect can be included by multiplying the term $[1 - (V/V_{i_0})^2]^{2/3}$ in Eq. 6 by the linearized $[1 - \alpha_1 (V/V_{i_0})^2]$ where α_1 is the fractional increase or decrease (if negative) in kC_D between $\Delta \rightarrow 0$ and $\Delta = M/\rho w$.
7. If $(L/D)_h$ and C_D vary significantly with V , for example, according to the linearized approximation

$$C_D(V) \cong C_D(V = \bar{V}_{i_0}^*) [1 + \delta (V - \bar{V}_{i_0}^*)]$$
and

$$(L/D)_h(V) \cong (L/D)_h(V = \bar{V}_{i_0}^*) [1 - \beta_1 (V - \bar{V}_{i_0}^*)]$$
then

$$(V_{i_0}^*)^2 \cong (\bar{V}_{i_0}^*)^2 [1 - (\delta - \beta_1) (V - \bar{V}_{i_0}^*)]$$
where, ordinarily, $\delta > \beta_1$. Where η_1 applies ($V \leq \bar{V}_{i_0}^*$), $V_{i_0}^* > \bar{V}_{i_0}^*$ and where η_2 applies ($\bar{V}_{i_0}^* < V$), $V_{i_0}^* < \bar{V}_{i_0}^*$. In either case the appropriate η exhibits a larger value than it would have without the δ and β_1 effect. Since $\delta - \beta_1$ is small, $V_{i_0}^* \cong \bar{V}_{i_0}^*$ in any event.
8. The algebra that results in Eq. 7 is based on an addition of Eqs. 2 and 3a (where, again, $M/\rho w$ is replaced by $[Mg - f_{DF} (L/D)_h]/\rho wg$ and A_p is accounted for in $(L/D)_h$) and a division of this sum by Eq. 3b with $(L/D)_h$ taken to be the fully loaded hydrofoil value and related to an arbitrarily loaded hydrofoil by the linearized (approximate) relationship $(L/D)_h$ (fully loaded) = $(L/D)_h \{1 - \beta [1 - (V/V_{i_0})^2]\}$.
9. Research supported entirely by Transportation Sciences Corporation, Los Angeles, California.

18 June 1968

13 DECEMBER 1968

Mercury's Rotation Period: Photographic Confirmation

Abstract. *Photographic measures of surface features on Mercury have led to a rotation period of 58.663 ± 0.021 days, which is in good agreement with the 58.646-day period required by a predicted 2:3 resonance between the axial and orbital periods. The incorrect interpretation of earlier visual and photographic observations which supported an 88-day rotation period appears to be partially explained by peculiar characteristics associated with the observability of various hermetic longitudes. The apparent contrast of most of the recorded surface features is marginal for visual observation when viewed through the terrestrial daytime sky. The intrinsic contrast of a relatively conspicuous feature was measured as 0.20, a value lower than that of typical markings observed on the moon and Mars.*

Throughout most of this century we have unhesitatingly accepted 88 days as the axial rotation period of the planet Mercury, or with somewhat less certainty 87.969 days, an interval precisely equal to its period of orbital revolution about the sun. This 88-day rotation period was first announced by Schiaparelli (1) after 8 years of visual observations through his modest telescope. Repeated confirmation was given (1) over the next several decades, but the matter was considered settled when Antoniadi published his support of the 88-day period (2). Still further confirmation was submitted by Dollfus (3) in the form of both visual and photographic evidence obtained at the French high-altitude observatory at Pic-du-Midi. The optical interpretation did not stand alone; theoretical arguments suggested that solar gravitational forces acting on a tidal deformation would lock Mercury's axial and orbital periods into synchronism in a manner similar to that of the moon in its orbit about the earth (2).

In 1965 Pettengill and Dyce announced that their radar observations of Mercury gave evidence for a rotation period of 59 ± 5 days (4). Furthermore Colombo suggested that the rotation period might be equal to exactly $2/3$ of the orbital period, or 58.646 days (5). While improved radar measures continued to converge on the 59-day period, several investigators found theoretical arguments which could account for Mercury's axial rotation being locked

into a 2:3 resonance with its orbital revolution (6).

A closer inspection was made of the earlier visual and photographic records, particularly the observations of Fournier, Antoniadi, Camichel, and Dollfus, which are generally considered to be the most reliable. Cruickshank and Chapman (7) found that certain visibility relations had combined in such a way that the historical records could support either the 88- or 59-day periods, although they assigned greater probability to the latter. Dollfus and Camichel (7) have reported recent visual observations which they contend are consistent only with a rotation period of 58.67 ± 0.03 days. Within the probable error, this period is in complete agreement with the 2:3 resonance condition. We would emphasize that to date all evaluations of the rotation period of Mercury have made use of recurrent appearances of recognizable features on the planet's surface; there are no references to direct quantitative observations of rotational motion.

We initiated our program of photography of Mercury in late 1965. As an object for telescopic photography, Mercury is among the most difficult in the solar system. Never appearing more than 27° (elongation angle) from the sun, its minute disk must usually be photographed in full daylight. Optimum observing geometry requires a compromise between phase and apparent size, and this occurs when the phase angle is approximately 70° . At this phase the elongation angle has an average value of 20° , and the disk is a mere 6 seconds of arc in diameter. The observational difficulty can best be expressed by the limit of our success over the past $2\frac{1}{2}$ years—a total of only 96 useful photographic plates on 64 different dates.

Until March of this year, the results of our photographic program were generally inconclusive, although a pair of plates taken on 6-8 May 1966 strongly suggested the 59-day rotation period. During March and April, however, we obtained several more plate sequences in which the daily rotational motion of several surface features across the disk of Mercury could be detected and measured. Rotation periods for four of these discrete surface features (tentatively labeled A, B, C, and D) are given in Table 1.

The observations summarized in Table 1 support the 59-day rotation period. Making use of the directly derived photographic rotation period,

one can substantially improve this accuracy through the use of an extended time base. Features A, B, and D, and two others (tentatively labeled E and F), were measured at intervals of one (B only) and 12 rotations of Mercury. With this improvement it was finally possible to make use of a 1942 photograph, taken some 160 rotations earlier at Pic-du-Midi, in which features E and F were identified and measured. Rotation periods derived from the recurrent appearances of features A, B, D, E, and F are given in Table 2. The weighted mean value for the rotation period is 58.663 ± 0.021 days (S.D.); the 58.646-day rotation period locked into a 2:3 resonance with Mercury's orbital revolution falls just within the computed error.

The crucial importance of the results in Table 1 should not be overlooked. Without the constraints imposed by these measures, the recurrent appearances listed in Table 2 would also support the 88-day rotation period.

All errors given in Tables 1 and 2 are statistical only and do not include any systematic errors that may arise out of photographic phase effects or uncertainty in the diameter of Mercury itself. Such systematic errors are probably the cause of the somewhat large rotation periods given in Table 1; however, it is to be expected that they would have a greatly reduced effect on the values given in Table 2. We have estimated that a reduction in the accepted diameter of Mercury of 5 percent would remove the discrepancy between Tables 1 and 2. However, uncorrected phase effects could just as likely be the cause.

We also investigated the observability conditions that might have led to the incorrectly inferred 88-day period. A computer program was prepared to give the hermographic longitude of Mercury's central meridian (δ), the longitude of the terminator, phase angle, elongation angle, ecliptic longitude, and several other parameters associated with the observability of the planet. Print-outs were obtained at daily intervals for all useful phase angles between 20° and

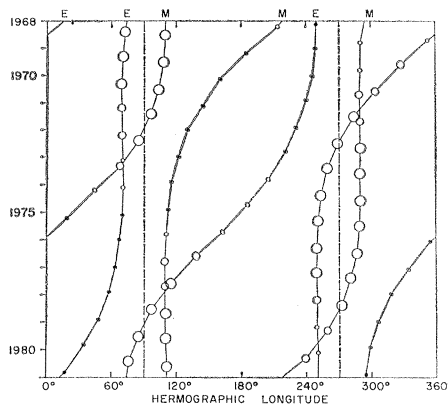


Fig. 1. Hermographic longitude of the center of the disk of Mercury at phase angle 70° for all evening (E) and morning (M) elongations throughout a 13-year cycle. Circle size indicates observational favorability for observatories in the Northern Hemisphere. An inverse relationship would apply to observatories in the Southern Hemisphere.

120° . The orbital periods of Mercury and the earth are such that 54 revolutions of Mercury are almost exactly equal to 13 revolutions of the earth. Therefore, the relative orbital positions of the two planets are repeated at 13-year intervals, and we were able to include all visibility geometry in a 13-year run from the computer program.

Using phase angle as a parameter of observability and selecting 70° as a mean value to represent each elongation, we listed the hermographic longitude of the central meridian and the ecliptic longitude of the planet for each of the 82 elongations (41 evening and 41 morning) that occur during a 13-year interval. The ecliptic carries Mercury alternately north and south of the celestial equator, and thus it was arbitrarily divided into four latitude zones with each being assigned an index of observability from 1 to 4. Thus, for observatories located in the Northern Hemisphere, the superiority of each elongation is determined by the ecliptic latitude: 1, excellent; 2, good; 3, fair; and 4, poor. For telescopes located in the Southern Hemisphere, the reverse listing would be appropriate. Figure 1

is a graphical representation of the results of this tabulation.

Several important characteristics of Mercury's selective visibility are immediately evident in Fig. 1. All elongations (both evening and morning), favorable to Northern Hemisphere observatories, tend to accentuate two specific longitudes— 90° and 270° (dashed lines)—with each being emphasized for somewhat more than half of the 13-year cycle. Thus, an observer in the Northern Hemisphere viewing only the favorable elongations would see essentially the same regions on Mercury for as long as 7 successive years. The regions around the longitudes of 0° and 180° are particularly unfavorable, being seen only under fair to poor conditions twice during the 13 years. It is now easier to understand why many observers might have concluded that Mercury presents a single hemisphere to the sun (88-day rotation period). For an observer in the Southern Hemisphere, however, all longitudes except those near 90° and 270° would be equally well presented and would be seen twice during each 13-year cycle. Therefore, the observable longitudes on Mercury shift rapidly from year to year for an observer in the Southern Hemisphere; had Schiaparelli or Antoniadi made their observations from Africa, Australia, or South America, the true rotation period of Mercury might have been established long ago.

In this analysis we have assumed that the observer can see only the hermographic longitude indicated by the location of the circle (Fig. 1). Such is not the case; not only can regions be studied as far as 40° from the central meridian (unless intercepted by the terminator), but moderately useful observations can be made over a range of phase angles extending from approximately 30° to 110° . Nevertheless, the longitudes indicated in Fig. 1 are typical of the regions most likely to reveal surface features under observing conditions which are less than ideal.

Another factor which must be taken

Table 1. Rotation periods derived from the motion of surface features across the disk of Mercury at intervals less than a single rotation.

Feature	Interval observed	Observations (No.)	Rotation period* (days)
A	25-31 March 1968	3	61.0 ± 0.6
B	23-28 March 1968	3	64.3 ± 2.0
C	28-31 March 1968	2	65.8 ± 5.0
D	6-8 May 1966	2	54.7 ± 11.0
D	5-13 April 1968	5	58.7 ± 1.5

* Weighted mean = 61.14 ± 1.68 .

Table 2. Rotation periods derived from the recurrence of surface features on the disk of Mercury at intervals of one or more rotations.

Feature	Interval observed	Observations (No.)	Rotation period* (days)
A	27 April 1966-28 March 1968	4	58.688 ± 0.045
B	27 April 1966-28 March 1968	5	58.696 ± 0.055
D	6 May 1966-13 April 1968	7	58.681 ± 0.015
E	10 August 1942-30 January 1968	3	58.652 ± 0.010
F	10 August 1942-30 January 1968	3	58.654 ± 0.011

* Weighted mean = 58.663 ± 0.021 .

into consideration when one attempts to explain the historical visual observations is the visibility or contrast of the features themselves and, consequently, the reliability of visual observations in general. McGovern, Gross, and Rasool (7), who studied several sets of visual observations, have concluded that Mercury's rotation period is 58.4 ± 0.4 days. While we fully agree with this conclusion, we strongly question the means by which they arrived at this result, since their rotation period was strongly influenced by four pairs of Antoniadi's observations (2). In examining the published drawings of Antoniadi, we find other observations which are in serious conflict with three of the pairs used by McGovern *et al.* Thus, the 59-day rotation period could be obtained by selecting only those observations which tend to support it, and by ignoring those which do not. We therefore conclude that at least some of the accepted visual observations are completely inaccurate, probably because of the marginal visibility of surface features on Mercury.

Photographs of Mercury taken in red light on 25 April 1968 show a well-defined feature of nontypical conspicuousness at 240° longitude located near the center of the disk. Photometric calibration applied to the photographic plates permits an evaluation of both the apparent and intrinsic contrasts of this marking. The value for the intrinsic contrast is about 0.20, somewhat less than the dark areas on the moon (0.4) and Mars (0.3 in yellow light). However, the apparent contrast of this feature is only 0.08, because Mercury was necessarily observed through the illuminated terrestrial daytime sky. Less conspicuous markings had contrasts less than half as great, and this certainly represents marginal visibility. Typical surface features on Mercury, therefore, are quite difficult to detect by direct visual observation. It remains for high-contrast photography to provide the most reliable means for mapping the surface of Mercury.

B. A. SMITH
E. J. REESE

Observatory, New Mexico State
University, Las Cruces 88001

References and Notes

1. G. Schiaparelli, *Astron. Nachr.* **123**, 242 (1890); Jarry Desloges, *Observations des surfaces planétaires* (F. Paillard, Abbeville, 1926), vol. 7; P. Lowell, *Mem. Amer. Acad. Arts Sci.* **12**, 431 (1902).
2. E. M. Antoniadi, *La Planète Mercure* (Gauthier-Villars, Paris, 1934).
3. A. Dollfus, *L'Astronomie* **67**, 61 (1953); *Planets and Satellites*, G. P. Kuiper and B. M.

Middlehurst, Eds. (Univ. of Chicago Press, Chicago, 1961), p. 534.

4. G. H. Pettengill and R. Dyce, *Nature* **206**, 1240 (1965).
5. G. Colombo, *ibid.* **208**, 575 (1965).
6. G. Colombo and I. I. Shapiro, *Smithsonian Astrophys. Obs. Spec. Rep.*, No. 188R (1965); *Astrophys. J.* **145**, 296 (1966); P. Goldreich and S. J. Peale, *Nature* **209**, 1078 (1966); W. H. Jefferys, *Science* **152**, 201 (1966).
7. W. E. McGovern, S. H. Gross, S. I. Rasool, *Nature* **208**, 375 (1965); D. P. Cruikshank and C. R. Chapman, *Sky Telescope* **34**, 24 (1967); C. R. Chapman, *Earth Planet. Sci. Lett.* **3**, 381 (1967); A. Dollfus and H. Camichel, *Compt. Rend.* **264**, 1765 (1967); H. Camichel and A. Dollfus, *Icarus* **8**, 216 (1968).

8. The prime meridian is defined as passing through the subsolar point at the instant of perihelion passage on 1 May 1968. The assumed 2:3 resonance between rotation period and orbital revolution would assure redefinition of the prime meridian at every other perihelion passage. We further assume that the rotation axis is perpendicular to the orbital plane.
9. We thank C. F. Knuckles, T. P. Pope, and A. S. Murrell who obtained the Mercury photographs, T. C. Bruce for programming, and the Computer Center of New Mexico State University for making CDC 3300 and IBM 1130 time available. Supported in part by NASA grants NsG-142-61 and NGR-32-003-027.

17 September 1968

Deficiency of Reduced Nicotinamide-Adenine Dinucleotide Oxidase in Chronic Granulomatous Disease

Abstract. *Reduced nicotinamide-adenine dinucleotide oxidase of normal human polymorphonuclear leukocytes has properties that would qualify it as the enzyme responsible for the respiratory burst during phagocytosis. The enzyme was deficient in leukocytes of five patients with chronic granulomatous disease. This lack of adequate reduced nicotinamide-adenine dinucleotide oxidase could be the basis for the metabolic abnormalities characteristic of these leukocytes and for their diminished bactericidal activity.*

When polymorphonuclear leukocytes phagocytize, they exhibit increased respiration, increased flow of glucose via the hexose monophosphate shunt (HMP) compared with that through the Embden-Meyerhof-Parnas pathway (1), and formation of hydrogen peroxide (2). The ingestion process itself and these metabolic concomitants are insensitive to cyanide (1), and the metabolic energy needed for the process has been considered to come from glycolysis (1).

In the phagocytic leukocytes of peripheral blood of children with chronic granulomatous disease (a genetic defect expressed as impaired intracellular killing of certain bacteria), the respiratory burst, the stimulation of glucose-6-phosphate oxidation, and formation of peroxide during phagocytosis are lacking (3), whereas the increase in glycolysis is normal. The leukocytes from these patients do ingest bacteria normally, but since they fail to kill many types of organisms, the patients suffer from various chronic infections (4). Attempts have been made to establish the reason (4) for the functional metabolic deficiencies in these leukocytes (5) and to define possible connections between these metabolic lacks and the inability of the cells to kill bacteria normally.

In any search for a key enzyme responsible for the respiratory burst of normal phagocytizing cells, the following must be kept in mind: (i) the enzyme should be insensitive to cyanide;

(ii) peroxide would probably be one of its products; (iii) the enzyme should be present in amounts adequate for the needs of the intact phagocytizing cell; and (iv) a relation between the respiratory enzyme and the hexose monophosphate pathway should be evident. There is evidence that the hexose monophosphate shunt itself is unimpaired in the patients' cells (3). Depression or lack of a terminal respiratory enzyme, which could be linked to the lack of bursts of respiration and HMP activity during phagocytosis, would not only indicate a key biochemical lesion in chronic granulomatous disease but would also help to establish that the enzyme is indeed responsible for the oxidative stimulations when normal cells phagocytize.

Recently, a flavoprotein enzyme, reduced nicotinamide-adenine dinucleotide (NADH) oxidase, was isolated and characterized from the soluble fraction of homogenates (prepared in isotonic KCl) from guinea pig peritoneal granulocytes (6). The enzyme is specific for NADH, and the products formed are hydrogen peroxide and nicotinamide-adenine dinucleotide (NAD⁺) in equimolar amounts (6). The enzyme is insensitive to cyanide and is present, at least in guinea pig polymorphonuclear leukocytes, in adequate amounts to cover the respiratory burst during phagocytosis. This enzyme thus would satisfy points (i), (ii), and (iii) above. Evidence is available which links this enzymatic activity (that is, NAD⁺ pro-